A. Murari, E. Peluso, M. Gelfusa, P. Gaudio, D. Mazon, N. Hawkes, G. Point,
B. Alper, T. Eich and JET EFDA contributors

A Method to Determine the Weights of Internal Magnetic Measurements for Optimised Equilibrium Reconstructions

A Method to Determine the Weights of Internal Magnetic Measurements for Optimised Equilibrium Reconstructions

A. Murari[1], E. Peluso[2], M. Gelfusa[3], P. Gaudio[3], D. Mazon[4], N. Hawkes[5],
G. Point[6], B. Alper[5], T. Eich[7] and JET EFDA contributors*

JET-EFDA, Culham Science Centre, OX14 3DB, Abingdon, UK

[1]*Consorzio RFX-Associazione EURATOM ENEA per la Fusione, I-35127 Padova, Italy.*
[2]*University of Rome 'La Sapienza', Piazzale Aldo Moro Rome Italy*
[3]*Associazione EURATOM-ENEA - University of Rome "Tor Vergata", Roma, Italy.*
[4]*Association EURATOM-CEA, CEA Cadarache, 13108 Saint-Paul-lez-Durance, France.*
[5]*EURATOM-CCFE Fusion Association, Culham Science Centre, OX14 3DB, Abingdon, OXON, UK*
[6]*Ecole Normale Supérieure de Cacahn- 61 Avenue du Président Wilson, 94230 Cachan, France*
[7]*Max-Planck-Institut für Plasmaphysik, Teilinstitut Greifswald, EURATOM Association,
Wendelsteinstr.1,17491 Greifswald, Germany*
** See annex of F. Romanelli et al, "Overview of JET Results",
(23rd IAEA Fusion Energy Conference, Daejon, Republic of Korea (2010)).*

ABSTRACT

In a Tokamak the configuration of the magnetic fields remains the key ingredient to improve performance. A method to choose the weights, to be given to internal measurements of the magnetic fields for improved equilibrium reconstructions, is presented. The approach is based on various statistical indicators applied to the residuals, the difference between the actual measurements and their estimates from the reconstructed equilibrium. In addition to the traditional analysis of the global distributions of the residuals, more sophisticated correlation tests have been performed. The potential of the method is exemplified using the measurements of the Faraday rotation derived from JET polarimeter. The magnetic reconstructions have been obtained with the code EFIT. The results indicate quite clearly that the weights have to be chosen carefully to strike the right balance between the quality of the reconstructions at the edge and in the core. The values of the weights have been shown to depend on the number of available measurements and their error bars. An inappropriate choice of the weights can have significant repercussions on the quality of the magnetic reconstruction both in the edge and in the core.

1. INTRODUCTION

Magnetic Confinement Nuclear Fusion (MCNF) relies exclusively on the configuration of the magnetic fields for the confinement and therefore for the maximisation of the plasma performance. In the last decades, more advanced configurations have been developed, such as hybrid modes, optimised shear etc, which require a carefully controlled shaping of the current profile. The accurate determination of the magnetic topology has therefore become even more crucial for both the running of the experiments and the scientific exploitation of the results [1].

In modern day Tokamaks, the magnetic topology is typically obtained, under the assumption of equilibrium between the magnetic and the kinetic pressure, solving the Grad-Shafranov equation [2]. The Grad-Shafranov equation is a two dimensional, nonlinear, elliptic partial differential equation, which has to be solved with some precautions. In any case, the reconstruction of the magnetic topology is an ill defined problem. The available measurements are typically compatible with different current profiles. In the case of advanced scenarios this problem is particularly severe and it has been recently demonstrated that magnetic internal measurements are indispensable to identify the more appropriate solutions among many at first sight reasonable candidates [3].

The only two measurement techniques, available to obtain indications about the internal topology of the magnetic fields in high temperature plasmas, are the Faraday rotation and the Motional Stark Effect (MSE). To introduce the methodology, the analysis has been focused on the Faraday measurements obtained with JET polarimeter. The diagnostic has been recently upgraded and calibrated with a new technique [4,5]. The quality of the measurements has therefore improved and this new data has been used as an input to the equilibrium code. It is worth noticing that, in any case, polarimetry is the most generally applicable technique to measure the internal fields. The diagnostic does not depend on the neutral beams and can be therefore used in any phase of

the discharge. Moreover it is expected to be more robust in terms of results and can be used in real time, as already demonstrated on JET [6]. It is also relevant that JET is the only present day device having an ITER-like configuration of the polarimeter, with 4 lines of sight seeing the plasma diagonally from the low field side (see figure 4).

On the other hand, notwithstanding the importance of the internal measurements to determine the magnetic topology, no principled technique is available to select the most appropriate weights to be given to the various measurements used as inputs. Traditionally, when EFIT is run with internal measurements, all the various inputs are given the same weights, independently from the nature of the measurements and their number. The least square minimisation takes into account only the error bars on the various measurements.

The indicators proposed in this paper are based on the analysis of the residuals, the difference between the actual measurements and the values recalculated on the basis of the reconstructed equilibrium. The most obvious indicator is of course the sum of the residuals. On the other hand, it can be easily demonstrated that, in the case of nonlinear systems, this simple quantity is not necessarily an adequate estimator. More advanced indicators, based on higher order correlations of the residuals have therefore also been applied [7-10]. The main idea behind the approach developed in this paper is the consideration that, if the reconstruction of the magnetic fields was perfect and the noise additive, the residuals should simply consist of noise. Therefore, in the case of additive white noise, the residuals should present the statistical distribution typical of this noise. Therefore the weights of the internal measurements can be determined by minimising not only the sum of the residuals but also statistical indicators, which have a minimum for the expected distribution of the residuals. The aforementioned main ideas can be formulated in rigorous mathematical terms, as described in detail in section 2.

To investigate the potential of the developed validation techniques, they have been applied to the main code used at JET for the magnetic reconstruction: EFIT [11]. This code solves the Grad-Shafranov equation and is briefly described in section 3, together with a short overview of the diagnostics providing the inputs and the ones used to validate the approach.

As expected, modifying the relative weights of the internal measurements, compared to the pick-up coils, reveals a tension between the reconstruction in the core and at the edge. The developed statistical indicators show that a reasonable trade-off can be found. The relative importance of the Faraday measurements can be increased up to the point where the reconstruction of the boundary is not significantly affected and the reconstruction of the core is significantly improved (see section 4). To increase the confidence in the conclusions, the quality of the calibrations has been checked using non magnetic measurements. Basically this has been done analysing IR measurements for the strike point position and the SXR emission for the core (sawteeth inversion radii). These aspects are discussed in section 5.

Summary and directions of future investigations are the subjects of the last section 6 of the paper. The statistical tools for the assessment of the optimal weights

2

2. THE STATISTICAL TOOLS FOR THE ASSESSMENT OF THE OPTIMAL WEIGHTS

By varying the relative weights of the internal measurements, compared to the pick-up coils, the resulting equilibria can be significantly modified. The quality of the results can be assessed first of all by calculating the sum of the residuals, the difference between the actual measurements and the values recalculated on the basis of the reconstructed equilibria. To take into account the quality of the measurements, it is normal practice to normalise the residuals of each type of measurement to the appropriate error bars. Therefore a general indicator of this type is of the form:

$$x = \sum_Q \frac{1}{n_s} \sum_{j=1}^{n_s} \frac{1}{N} \sqrt{\frac{\sum_{i=1}^{N} \left((Q_{rec.}(t_i))_j - (Q_{meas.}(t_i))_j \right)^2}{\sigma_Q^2}} \tag{1}$$

Where Σ_Q is the sum over the physical quantities Q, both measured ($Q_{meas.}$) and reconstructed ($Q_{meas.}$); n_s stands for the number of measurements (probes or chords). Finally N_i is the number of time points used for each discharge and the statistical error of the quantity analysed is σ_Q.

Indicators, of the form of equation (1), will be used in the following to assess the quality of the equilibria because they are familiar and easy to calculate. On the other hand, it is well known that, for nonlinear systems, a simple parameter such as χ is not guaranteed to provide the right answer. A correlation analysis of the time evolution of the residuals is on the contrary a much more reliable quantifier as shown in [7-10]. The main idea is to apply whiteness tests, statistical tests, which assess how close the distribution of the residuals is to white noise. The combination of weights, which provides the residual distribution closer to white noise, is to be preferred. The approach of the residual autocorrelations to model validation, just described in intuitive terms, can be formulated as a statistical hypothesis testing problem [12]. In our case, the application of these criteria is simpler. The more appropriate choice of the weights is the one corresponding to the minimum of the two autocorrelation functions described in the following.

In mathematical terms, consider a general Multi-Input and Multi-Output (MIMO) discrete time model representation:

$$\vec{y}(t) = \vec{f}(\vec{y}^{\,t-1}, \vec{x}^{\,t-1}, \vec{\varepsilon}^{\,t-1}) + \vec{\varepsilon}(t) \tag{2}$$

where t ($t = 1,2,...$) is a time index and $\vec{y}(t)$, $\vec{x}(t)$ and $\vec{\varepsilon}(t)$ denote, respectively, the dependent variable, independent variable and residual vectors. $\vec{f}(\cdot)$ is a vector non-linear function:

$$
\begin{aligned}
\vec{y}(t) &= \left[y_1(t),...,y_q(t) \right]^T \\
\vec{x}(t) &= \left[x_1(t),...,x_r(t) \right]^T \\
\vec{\varepsilon}(t) &= \left[\varepsilon_1(t),...,\varepsilon_q(t) \right]^T \\
\vec{f}(t) &= \left[f_1,...,f_q \right]^T
\end{aligned}
\tag{3}
$$

where q is the number of dependent variables and r is the number of independent variables.

An adequate set of tests for a nonlinear, MIMO system is provided by the higher order correlations between the residuals and input vectors given by the following two relations:

$$\o_{\xi\eta}(\tau) = E\left[\xi(\tau)\eta(t+\tau)\right] \tag{4}$$

$$\o_{\vartheta\eta}(\tau) = E\left[\vartheta(\tau)\,\eta\,(t+\tau)\right] \tag{5}$$

where $\xi(\tau)$ is the residuals vector, $\eta(\tau)$ the vector of the outputs time their residuals and $\vartheta(\tau)$ the inputs vector. In the previous relations E is the operator indicating the expectation (average) operation. So these vectors can be calculated as:

$$\xi(t) = \varepsilon_1^2(t) + ... + \varepsilon_q^2(t) \tag{6}$$

$$\eta(t) = y_1(t)\,\varepsilon_1(t) + ... + y_q(t)\,\varepsilon_q(t) \tag{7}$$

$$\vartheta(t) = u_1^2(t) + ... + u_r^2(t) \tag{8}$$

If the non linear model is an adequate representation of the system, in the ideal case, equations (4) and (5) applied to the residuals should give:

$$\o_{\xi\eta}(\tau) = \begin{cases} k, & \tau = 0 \\ 0 & otherwise \end{cases} \tag{9}$$

$$\O_{\vartheta\eta}(\tau) = 0, \forall\,\tau \tag{10}$$

where k is a constant, equal to:

$$k = \frac{\left(\sum_{t=1}^{N}(\xi_{norm}(t))^2\right)^{1/2}}{\left(\sum_{t=1}^{N}(\eta_{norm}(t))^2\right)^{1/2}} \tag{11}$$

If the correlations in (4) and (5) remain within the 95% confidence interval of the values given by the equations (9) and (10), then it is reasonable to consider the model adequate. On the contrary, if the correlations exceed this value, the model is to be considered somehow defective.

The previous equations have to be particularised for our case of equilibrium reconstruction. As shown in [12], an appropriate definition of inputs and outputs in the case of EFIT is the one illustrated graphically in figure 1. So the inputs to EFIT are the various measurements available and the outputs are the estimates of the same measurements, calculated on the basis of the fields reconstructed by EFIT. The minimum of these correlations, expressed by relations (4) and (5), are expected to indicate the optimal set of weights to be given to the available measurements.

3. OVERVIEW OF THE RECONSTRUCTION CODES AND THE DIAGNOSTICS

3.1 CODES

The reconstruction of the plasma equilibrium in a Tokamak is a free boundary problem. The plasma boundary is defined as the last closed magnetic flux surface; inside the plasma, the equation expressing the equilibrium between the magnetic and the kinetic pressures in an axisymmetric configuration is the Grad-Shafranov equation. This equation is derived from the combination of the magnetostatic Maxwell's equations, which are satisfied in the whole space in presence of a magnetic field, and the equilibrium of the plasma itself, which is assumed to occur when the kinetic pressure is equal to the Lorentz force of the magnetic pressure.

The Grad-Shafranov equation can be expressed in the following form:

$$-\Delta^*\psi = rp'(\psi) + \frac{1}{\mu_0 r}\ (ff')(\psi) \tag{12}$$

in which μ_0 is the magnetic permeability of the vacuum, $\psi(r,z)$ is the poloidal flux, $p(\psi)$ is the plasma pressure, $f(\psi)$ the diamagnetic function and prime indicates derivative with respect to the poloidal flux ψ. Δ^* is the linear elliptic operator defined as:

$$\Delta^* = \frac{\partial}{\partial r}\left(\frac{1}{\mu r}\frac{\partial}{\partial r}\right) + \frac{\partial}{\partial z}\left(\frac{1}{\mu r}\frac{\partial}{\partial z}\right) \tag{13}$$

The main equilibrium code use on JET is EFIT, which is the one used to obtain the reconstructions of the magnetic fields discussed in this paper. More information about this code is provided in the next subsection. The reference code for the determination of the last closed magnetic surface at JET is XLOC; the main characteristics of this code are presented later in this section. It can be considered a reference for the quality of the boundary reconstructions in JET.

EFIT (Equilibrium Fitting) is a computer code that was developed to obtain the topology of the plasma internal magnetic fields and the boundary on the basis of the measurements available. The magnetic measurements used as inputs by EFIT are obtained from two different types of diagnostics: a) external-passive: such as magnetic probes and poloidal flux loops; b) internal-active: the Faraday rotation and the Motional Stark Effect (MSE).

The Grad-Shafranov equilibrium equation is solved using the available measurements as constraints on the toroidal current density. Since the current also depends on the solution of the Grad-Shafranov equation, the poloidal flux function, equation (12) represents a nonlinear optimization problem. The code determines the source term in the non linear Grad-Shafranov equation by a least-square minimization of the difference between the measurements and their estimates derived from the reconstructed fields. From a conceptual point of view therefore, the problem is thus reduced to finding a solution that minimizes a cost function of the type:

$$J(\psi) = J_0 + K_1 J_1 + K_2 J_2 + K_3 J_3 + K_4 J_\varepsilon \tag{14}$$

with:

$$J_0 = \sum_i \left(\frac{1}{r} \frac{\partial \psi}{\partial n} (N_i) - g_i \right)^2$$

$$J_1 = \sum_i \left(\int c_i \frac{n_e}{r} \frac{\partial \psi}{\partial n} \, dl - \alpha_i \right)^2$$

$$J_2 = \sum_i \left(\int c_i \, n_e \, dl - \beta_i \right)^2$$

$$J_3 = \sum_i \left(mse_i - \gamma_i \right)^2$$

(15)

where g_i, ψ_i and β_i are respectively the measurements of the magnetic poloidal field, the Faraday rotation and the line integrated density along the chords C_i. In (15) mse_i indicates the reconstructed measurement of the motional Stark effect at point i. The weighting parameters K_1 to K_4 enable to give more or less importance to the corresponding experimental measurements.

The results presented in this paper have been obtained with the well known EFITJ code described in detail in [13]. This version of EFIT contains an iron core model validated with a series of tests also reported in [13]. It has been chosen to run EFIT using a cubic spline having nine knots for the p' and ff' profiles. The border conditions for those profiles are zero. The detailed, optimised weights used for the various pick-up coils are also given in [13]. Two details of the implementation are important for the scope of this paper. First of all relations (14) and (15) are not implemented exactly in the way reported. All the various measurements are multiplied by individual coefficients to allow maximum flexibility. Secondly, these coefficients can assume a value only in the interval [0,1]. Therefore, in order to increase the weights of the polarimetric measurements compared to the magnetic coils, the only option is to decrease the coefficients multiplying the coils. Since in JET the relative weights of the various coils have already been subject of a very long optimisation process, in the analyses reported in this paper, all the coils are multiplied by exactly the same coefficient K_0 varying in the interval [0,1]. The value $K_0 = 1$ is the case in which the measurements are all attributed the same weights with a correction only for their different error bars.

The second code, whose results are utilised in this paper, is called XLOC [11]. XLOC was originally introduced on JET in order to provide a fast and accurate determination of the plasma boundary in the neighbourhood of the X-point. This method has been extended to cover the whole plasma boundary and XLOC now routinely provides the boundary for arbitrary plasma configurations. It is also used for plasma shape real-time control on a daily basis. From this code, the main parameters of JET boundary, like the strike point position and the distance from the wall, are determined with a time resolution better than 1ms. Nowadays, after an extensive use and benchmarking with other diagnostics, XLOC provides the most reliable and precise determination of the plasma boundary on JET and is therefore considered the reference code in this respect. On the other hand, with this algorithm it is not possible to compute the internal magnetic flux configuration.

3.2 DIAGNOSTICS

The main diagnostics used for the tomographic reconstructions reported in this paper are pickup coils measuring the local magnetic field. A pickup coil consists of a single-turn or multiple-turn coil of wire, used to measure the component of the local magnetic field perpendicular to the plane of the coil. The output voltage is proportional to the time derivative of the average magnetic flux linked with the windings. There are several measuring coils subsystems at JET, located in different poloidal and toroidal positions. On JET the main types of coils are flux loops, saddle coils and small pickup coils. The reconstructions of the equilibrium reported in this paper have been obtained with a set of 4 flux loops and a set of 27 saddle coils. Several systems of pickup coils are installed on JET. Each system is typically classified according to its position around the plasma as shown in figure 2. The 135 coils placed inside the in vacuum vessel wall are located in 18 different poloidal positions at 8 toroidal angles. Two different sets of divertor coils, for a total amount of 72, are located in the divertor region. Finally, there are 3 inner coils placed in the inner region outboard the plasma, 56 outer poloidal limiter coils in the region on the vessel outboard the plasma and 27 upper coils fitted in the upper part of the vessel. The results reported in this paper have been obtained by EFIT and XLOC, using a part of all pickup coils available, located in the same poloidal cross section. The positions and names of the coils used in this work are listed in [12]. All the coils on JET have been tested systematically and are considered to be affected by errors of the order of a few percent of the measured value.

To assess the impact of the coil weights on the quality of the boundary reconstruction, the estimates of EFIT have been compared to XLOC outputs. The code XLOC expresses the distance between the last closed magnetic surface and the wall in terms of discrete distances at specific poloidal positions called gaps. Some of these gaps have been analysed and are listed in table 1. The location of the coils and gaps used in this work is reported in figures 3.a and 3.b. The magnetic topology determined by EFIT can be used to calculate the same gaps and the two estimates can be compared.

The other main diagnostic, whose data have been used to obtain the results reported in this paper, is JET polarimeter. If a linearly polarized electromagnetic wave is sent into a magnetized plasma the following effects occur:

1. Faraday rotation of the polarization plane, proportional to the density times the magnetic field component parallel to the direction of the laser beam propagation.

2. Cotton–Mouton phase shift, proportional to the density times the square of the magnetic field component perpendicular to the propagation direction.

These effects can be described by the following equations:

$$\Delta\Psi \propto \lambda^2 \int n_e \cdot B_\parallel \cdot dz \tag{16}$$

$$\Phi \propto \lambda^3 \int n_e \cdot B_\perp^2 \cdot dz \tag{17}$$

In equations (16) and (17), λ is the laser wavelength, n_e is the plasma electron density and $B_\parallel$ and $B_\perp$ the parallel and perpendicular components of the magnetic field respectively. To summarise, traversing a magnetised plasma, a polarised beam suffers a rotation of the polarisation plane due to Faraday Rotation and acquires ellipticity due to the Cotton-Mouton effect.

On JET, the FIR diagnostic operates as a dual interferometer/polarimeter [4,5]. The system probes the plasma with 4 vertical and 4 lateral laser beams. The diagnostic provides the line-integrated plasma density measurements, by means of interferometry and Faraday rotation angle, and Cotton-Mouton phase shift measurements by polarimetry. These measurements are preceded by an on-line calibration procedure performed before each shot (using half-wave plates). The calibration of the polarimetric measurements has been significantly improved in the last couple of years [4,5]. The quality of the measurements is therefore higher than in the past and now an accuracy of about 10% can certainly be achieved. The layout of the instrument lines of sight is shown in figure 4. Due to instrumental issues, the polarimetric chords of good quality available to perform the analysis described in this paper are number 3,5 and 7.

The previous diagnostics measure basically the magnetic fields. To confirm the conclusions of the magnetic analysis, other diagnostic data has been used. The two most useful have proved to be infrared thermography and the diodes for the measurements of the Soft X-ray emission (SXR).
In the last years, the emphasis of the studies of plasma wall interactions on JET has motivated the installation of a series of IR cameras. One of the most advanced is a camera located on top of the machine to perform thermography studies in the JET divertor. The layout of the diagnostic and the view of the divertor are provided in figure 5. The system can measure the emission from the outer strike point and therefore determine its position. The camera has a very high frame rate and is coupled to infrared optics which provide a spatial resolution of the order of a few mm. Given some additional uncertainties, mainly linked to the vibrations of the machine during ELMs, the accuracy in the determination of the strike point position is certainly not worse than 10 mm.
JET is also equipped with a number of cameras hosting tens of Si diodes for measurements of the SXR emission and tomographic reconstruction. These diodes are unfortunately quite vulnerable to radiation damage. Therefore, even if they have been shielded, they are damaged quite frequently, particularly during high power sessions. In the last years many three cameras have remained operational and they are shown in figure 6. They are located in different toroidal cross sections and therefore do not really allow tomographic reconstruction. On the other hand they can provide quite reliably useful information such as the position of the inversion radii of the sawteeth, as discussed in more detail in section 5.

The analysis of the results has been performed using a validated database of about 10 JET discharges. The choice has been mainly driven by the availability of the diagnostics so these discharges are not expected to be biased and cover a quite representative fraction of JET operational space. This analysis is therefore considered more than adequate to show the potential of the

methodology proposed in the paper. For more specific physical studies the approach could be of course particularised for the required configurations (of both the plasma and the available diagnostics; see also section 6).

Finally, the time interval analysed for each pulse is the steady state phase of the discharges. Transient phases in principle do not present any conceptual problem. The same approach and in particular exactly the same indicators can be used also to investigate transients. On the other hand the measurements on JET are typically of better quality during the steady state part of the discharge and therefore this is the phase which has been studied in this paper to introduce the potential of the method.

4. STATISTICAL ANALYSIS USING THE MAGNETIC MEASUREMENTS

First of all, the statistical indicators briefly described in section 2 have been applied to the all the residuals of the measurements used as inputs to EFIT. In this case, equation (1) becomes

$$x = x_{Magnetic} + x_{Faraday} \tag{18}$$

In the previous equation the has been computed using the Pick-up coils, the Saddle ones and the magnetic fluxes; while the includes the Faraday rotations only.

In more detail equations (1) and (2) can be particularised as:

$$x_{Magnetic} = \frac{1}{n_{Pick\text{-}up}} \sum_{j=1}^{n_{Pick\text{-}up}} \frac{1}{N} \sqrt{\frac{\sum_{i=1}^{N} \left((B_{rec.}(t_i))_j - (B_{meas.}(t_i))_j \right)^2}{\sigma_B^2}} +$$

$$+ \frac{1}{n_{Saddle}} \sum_{j=1}^{n_{Pick\text{-}up}} \frac{1}{N} \sqrt{\frac{\sum_{i=1}^{N} \left((B_{rec.}(t_i))_j - (B_{meas.}(t_i))_j \right)^2}{\sigma_S^2}} + \tag{19}$$

$$+ \frac{1}{n_{Flux}} \sum_{j=1}^{n_{Flux}} \frac{1}{N} \sqrt{\frac{\sum_{i=1}^{N} \left((\phi_{rec.}(t_i))_j - (\phi_{meas.}(t_i))_j \right)^2}{\sigma_\phi^2}}$$

$$x_{Faraday} = \frac{1}{n_{Faraday}} \sum_{j=1}^{n_{Faraday}} \frac{1}{N} \sqrt{\frac{\sum_{i=1}^{N} \left((\vartheta_{rec.}(t_i))_j - (\vartheta_{meas.}(t_i))_j \right)^2}{\sigma_\vartheta^2}} \tag{20}$$

The different physical quantities (Q) used, both measured ($Q_{meas.}$) and reconstructed ($Q_{rec.}$) by EFIT, have a statistical error indicated by σ_Q. In the previous equation (n_Q) stands for the number of samples (probes or chords) used for each quantity; while the number of points used for each shot is N.

The statistical errors used are the 3% of the measured magnetic field for the Saddle and for the Pick-up coils, $\sigma_\phi = 20mWb$ for the flux loops and $\sigma_\vartheta = 0.20deg$ for the Faraday rotation measurements. These values are the best estimates provided by the diagnostic experts for the considered discharges.

The χ indicator has been calculated for different values of the weights given to the magnetic coils, decreasing their importance compared to the Faraday rotation measurements. As mentioned

in section 3, in order not to introduce any spurious effects, the weights of the magnetic coils have been multiplied all by exactly the same factor K_0. The trend of the normalised χ indicator with this K_0 multiplicative factor is shown in 7, for subset of the investigated discharges for clarity sake. The most appropriate value for the χ indicator is typically in the range of K_0 between 0.2 and 0.3 (where χ reaches a minimum).

The same analysis has been performed for the non linear global correlations of the residuals to cross check the results obtained using the χ indicator.

As mentioned in section 2, for each physical quantity studied, the characteristic MIMO analysis has been performed. The absolute values of the Non Linear Autocorrelation Global Functions (NACGF) have been added together and then subtracted to the maximum value acceptable for the 95% of confidence level, as follows:

$$Res_{\xi\eta} = \left(\sum_{i}^{N} | \phi_{\xi\eta}(t_i) | \right) - 1.96 \sqrt{N} \tag{21}$$

$$Res_{\theta\eta} = \left(\sum_{i}^{N} | \phi_{\theta\eta}(t_i) | \right) - 1.96 \sqrt{N} \tag{22}$$

These quantities have been computed for each K_0. The value of K_0 giving the smallest $Res_{\xi\eta}$ and $Res_{\theta\eta}$ is considered the most appropriate.

In table 2 the results of the analysis performed using χ and NACGF have been reported for the pulses analysed.

The results of table 2 indicate quite clearly that the quality of the reconstructions improves if the weights of the Faraday rotation measurements are increased compared to the coil measurements, in other words, if the magnetic' weights are reduced without modifying the Faraday' ones. This is not surprising since the number of chords available, only 3, is very limited and therefore it is advantageous to increase their importance. The analysis also seems to give quite consistent results and indicates that the optimal weights are in the interval 0.2 - 0.3. Given the fact that the two types of indicators are independent, this is a quite reassuring outcome of the analysis.

For the interpretation of these results, it is useful to particularize the analysis for the magnetic measurements and the Faraday rotations. In the figures 8 the individual terms in equations (18) are shown again for some representative discharges.

Analysing separately the residuals of the magnetic measurements and the Faraday rotations reveals a tension between the reconstruction of the core and the edge. Increasing the weights of the polarimetric measurements improves the reconstruction in the core. The quality of the edge, on the contrary, is not affected initially but when the weights of the magnetic are reduced below about 0.2-0.3, the boundary is too affected and the quality of the whole equilibria is of lower quality. It is worth motioning that for $K_0 = 0.1$ EFIT very often does not manage to converge. Therefore the fact that the statistical estimators indicate a lower quality of JET equilibria for such a low value of K_0 is confirmed by this difficulty of the code to converge. Also a visual inspection of the equilibria

10

confirms that values of K_0 below 0.2 are not acceptable.

The previous indications can be confirmed by comparing EFIT reconstruction of the boundary with the one obtained with XLOC. As can be seen in figure 10, using $K_0 = 0.3$ the reconstruction of the plasma boundary is not heavily affected.

5. CONFIRMATION OF THE RESULTS WITH DIFFERENT SETS OF MEASUREMENTS AND NON MAGNETIC MEASUREMENTS

A first test to confirm the results reported in the previous section consists of analysing how the optimum coefficient K_0 varies with the number of coils available. To this end, EFIT has been run with a different number of coils to assess whether the variations in the optimal value of K_0 are coherent with expectations, i.e. the value of K_0 should increase if the number of coils is reduced. An example, obtained eliminating about 30% of the coils, is shown in figure 11. Decreasing further the number of coils is not an option because with even fewer coils EFIT tends not to converge any more. Figure 11 proves very clearly that if the number of coils changes, compared to the number of polarimetric chords, the indicators identify a different optimal coefficient K_0. The behavior of the χ indicator shows clearly that reducing the number of probes, the best value becomes $K_0 = 0.3$ instead of 0.2. A similar behavior can be seen in Figures 12 for Pulse No: 73344. In this second case the reduction in the number of coils is such that χ presents a comparable value at both $K_0 = 0.3$ and $K_0 = 0.4$ instead of presenting a clear minimum at $K_0 = 0.3$.

Another series of tests have been aimed at verifying the results with non magnetic measurements. This is not an easy task since there are only very few non magnetic measurements on JET, with the available space resolution to constitute a good benchmark of the magnetic reconstructions. To support the conclusions about the quality of the boundary, and in particular the fact that it is not significantly degraded if a value of $K_0 = 0.3$ or $K_0 = 0.2$ is chosen, the best results have been obtained comparing the outer strike position identified by EFIT with the one obtained by IR thermography. From the footprint of the plasma, as seen by the camera described in section 3.2, it is possible to determine the position of the outer strike point. This is a geometrical parameter which can be compared with the estimate of EFIT for the various weights.

In Figures 13 and 14 the strike point positions identified by EFIT, using $K_0 = 0.1$, $K_0 = \{0.2$ or $0.3\}$ and $K_0 = 1$ and by the IR termography are shown. Since EFIT tends to overestimate the radius of the strike point, for clarity sake in the figure the lowest limits of the EFIT estimates have been compared with the IR estimate. The error bars used to plot the results in the figures are 4 cm for the EFIT reconstructions and 1 cm for the IR determination of the strike point position.

The results, shown graphically in Figures 13 and 14, confirm the previous conclusions. Lowering the K_0 parameter down to about 0.3 or 0.2 does not affect significantly the quality of the EFIT determination of the outer strike point position. Decreasing further the weights of the magnetic measurements, the discrepancy between the EFIT and the IR estimate decreases significantly and reaches unacceptable values.

To confirm the improvement in the quality of the core plasma reconstruction, once the weights of the Faraday rotation measurements are increased, the most reliable results have been obtained using the Soft X-rays (SXR) measurements. The arrays of SXR detectors in JET allow determining the inversion radius of sawtooth instabilities. The inversion radii are to be compared with the EFIT positions of the surface in the equatorial plane. The agreement between the SXR based estimates and the ones derived from EFIT can be quantified with the following indicator:

$$\chi = \frac{1}{2N}\sqrt{\sum_{i=1}^{N}\left[(R_{HF}^{SXR}(t_i) - R_{HF}^{EFIT}(t_i))^2 + (R_{LF}^{SXR}(t_i) - R_{LF}^{EFIT}(t_i))^2\right]} \qquad (23)$$

In the previous equation the subscript "HF" stands for High Field side, while "LF" for Low field side; moreover, "SXR" stands for Soft X-Rays and EFIT for the position computed interpolating with a cubic spline, the $q(R, t)$ profile in order to find the position of the $[q(R, t)|]_{t\to fixed} = 1$.

As already explained using the HF and LF side radii of the surface $q(R) = 1$ and those provided by the SXR emission for the same rational surface, it has been possible to obtain the behavior shown for the Pulse No: 75724. Again the results of the previous section, based on the magnetic measurements only, are also confirmed. The improvements in the reconstruction of the magnetic topology in the core increases constantly as the weights of the polarimetric measurements are increased (as usual down to a value of K_0 of 0.2). This is shown in Figure 15.

To summarize, double-checking the quality of the magnetic topology, using non magnetic measurements, confirms that, for the discharges of the database, a reasonable tradeoff is the use of a weight K_0 between 0.3 and 0.2.

DISCUSSION, CONCLUSIONS AND FURTHER DEVELOPMENTS
Two different classes of indicators have been used to quantify the quality of the magnetic topology when the weights of the internal measurements of the field are varied. The first class of indicators is of the χ type, in the sense that it quantifies the sum of the residuals weighted by the uncertainties in the measurements. The second class of estimators consists of high order correlation function, to quantify the statistical correlations of the residuals. They are basically whiteness tests adequate to non linear systems. Both types of indicators agree that the polarimetric measurements should have approximately weights, which are about three times the ones of the magnetic pickup coils.
The described investigations have shown that there is a tension between the quality of the reconstructions at the edge and in the core. Increasing the weights of the polarimetric measurements improves the reconstruction in the core but attention is to be paid not to degrade the quality of the boundary. Fortunately it seems possible to find an acceptable trade-off, which for, the discharges considered, consists of choosing a value of K_0 between 0.3 and 0.2.
It is worth pointing out that the estimators used in the paper are quite general. The approach is therefore of wide applicability and can be used to study other aspects of the equilibrium. A similar methodology could for example be adopted to determine the most appropriate weight to be given

to the constraint of the pressure. The effect of additional polarimetric measurements, in particular of chord 4, would also be interesting. In the future it is also planned to apply the same approach to discharges in which also the measurements of the MSE are available. Another interesting line of research would consist of investigating to what extent the optimal weights to be given to the internal measurements change with the plasma configuration.

REFERENCES
[1]. J. Wesson "Tokamaks" Clarendon Press, Oxford, third edition, 2004

[2]. Lao, et.al., Nuclear Fusion **30**, 1035 (1990).

[3]. F.S. Zaitsev, D.P. Kostomarov, E.P. Suchkov. Existence of substantially different solutions in an inverse problem of plasma equilibrium reconstruction. 35th EPS Plasma Physics Conference. Crete, Greece, 2008. P-1.091, 4p. (http://epsppd.epfl.ch/Hersonissos/pdf/P1_091.pdf).

[4]. M. Gelfusa et al Review of Scientific Instruments **81**, 1 (2010) F

[5]. M. Gelfusa et al Measurement Science and Technology **21** (2010) 115704 (11pp)

[6]. D. Moreau et al., "Development of Integrated Real-Time Control of Internal Transport Barriers in Advanced Operation Scenarios on JET", in Fusion Energy 2004 (Proc. 20th Int. Conf. Vilamoura, 2004) (Vienna: IAEA) CD-ROM file EX/P2-5 and http://www-naweb.iaea.org/napc/physics/fec/fec2004/datasets/index.html

[7]. S.A. Billings, and W.S.F. Voon, "Correlation based model validity tests for non linear models", International Journal of Control, **44**, 1986, pp. 235-244.

[8]. S.A. Billings and Q.H. Tao, "Model validity tests for non-linear signal processing applications", International Journal of Control, **54** 1, 1991, pp. 157-194.

[9]. S.A. Billings and Q.M. Zhu, "Model validation tests for multivariable non-linear models including neural networks", International Journal of Control, **62** 4, 1995, pp. 749-766.

[10]. S.A. Billings and W.S.F. Voon, "Structure detection and model validity tests in the identification of nonlinear system", Proceeding of the institution of electronic engineers, Pt D, Vol **130**, 1983.pp. 193-199.

[11]. D.P. O'Brien, J.J. Ellis and J. Lingertat Nuclear Fusion **33** (1993) 467

[12]. A. Murari et al Nuclear Fusion **51** (2011) 053012 (18pp)

[13]. D.P. O'Brien, et al, "Equilibrium Analysis of Iron Core Tokamaks Using a Full Domain Method," 1992 Nuclear Fusion **32** 1351.

Geometrical parameters used	
XLOC name	**EFIT name**
TOG 3	GAP 1
GAP 2	GAP 2
GAP 3	GAP 3
GAP 4	GAP 4
LOG	GAP 5
GAP 6	GAP 6
GAP 7	GAP 7
ROG	ROG
RIG	RIG
ZUP	ZUP

Table 1: Names of the different geometrical parameters used for comparison.

Shot number	χ	**NACGF**
73340	0.2	0.2
73344	0.3	0.3
73660	0.3	0.3
73920	0.2	0.2
74366	0.3	0.3
75724	0.3	0.2
79755	0.3	0.3
79756	0.2	0.2

Table 2: Results for the shot analysed showing the best K_0 using the χ indicator and the non linear (NACGF) autocorrelation functions.

Input:
Measurements of the magnetic field   u →

EFIT

→ y   **Output:**
EFIT - calculated magnetic field measurements

JG11.244-1c

↑
ε
Residuals:
Difference
between measurements & EFIT
estimates of the measurements
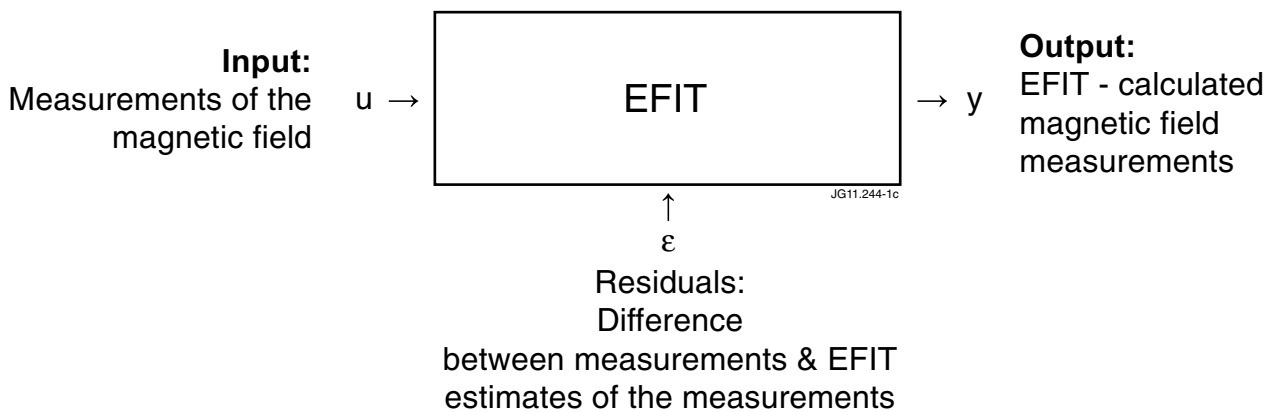
Figure 1: application of the correlation analysis of the residuals to the equilibrium code EFIT.
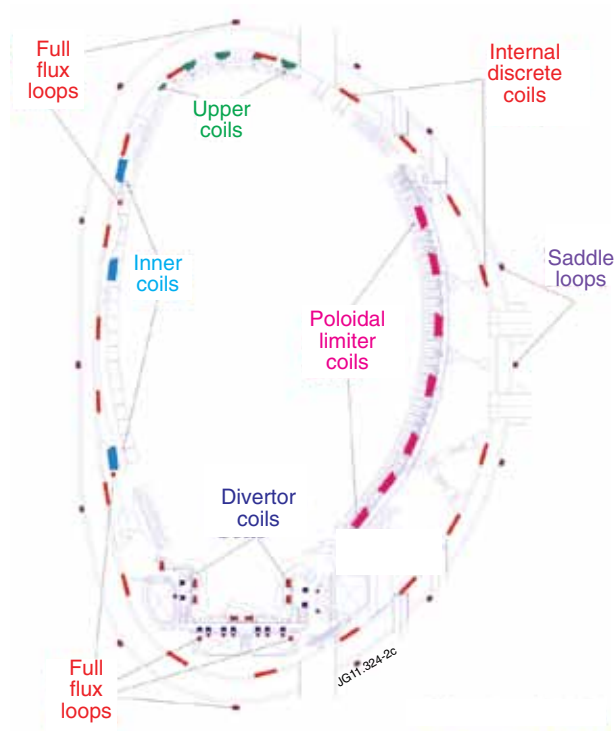
Figure 2: Equilibrium Magnetics: Pick-up coils and Flux Loops.
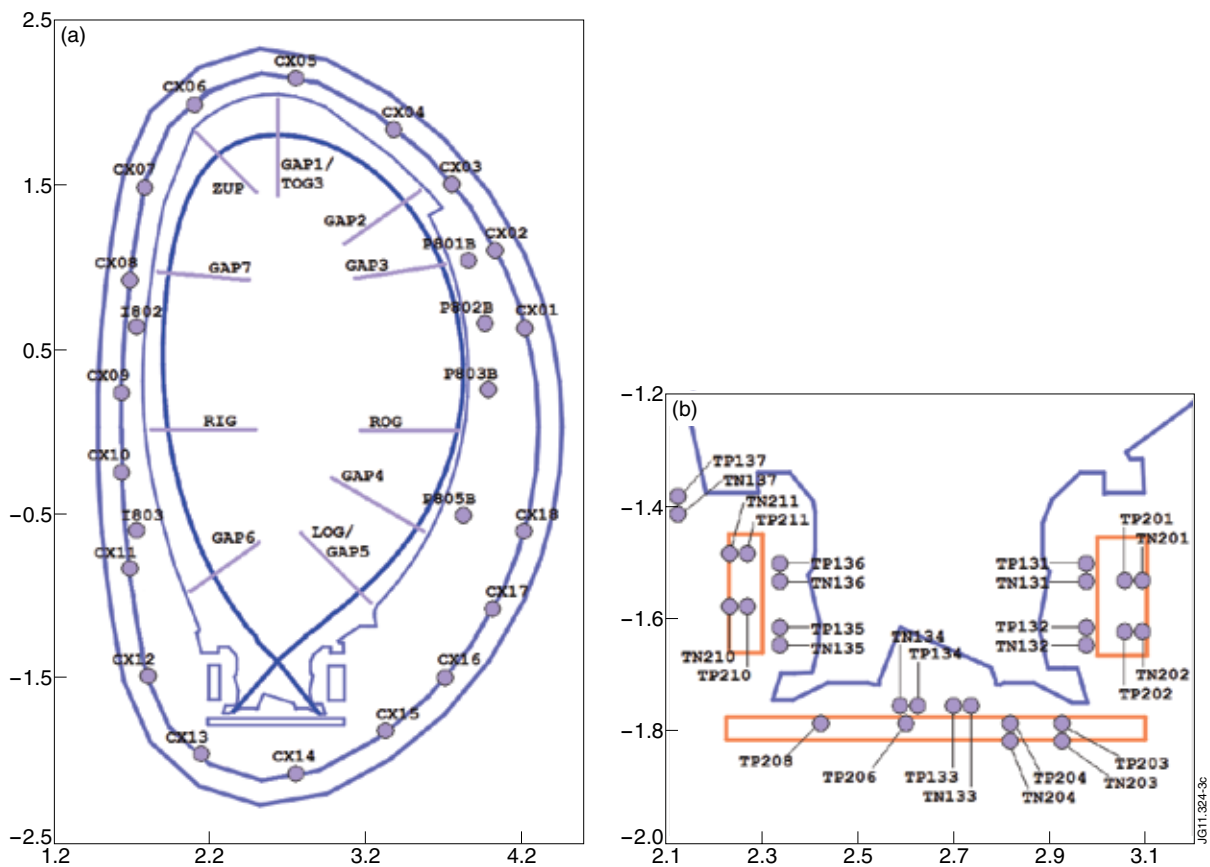
Figure 3: (a) Position of the gaps and the pickup coils around the first wall, divertor coils excluded. The dark blue curve represents the last closed magnetic surface of a possible plasma shape.

Figure 3: (b) Position of the pickup coils in the divertor region.
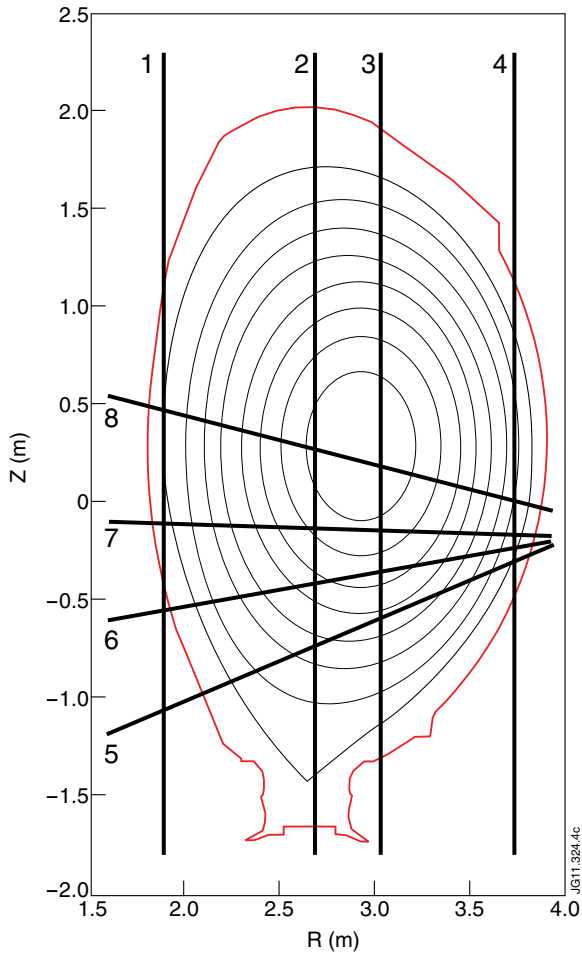
Figure 4: the layout of JET polarimeter lines of sight.

SchnittB-B
Iris with 16mm hole
View without vignitation
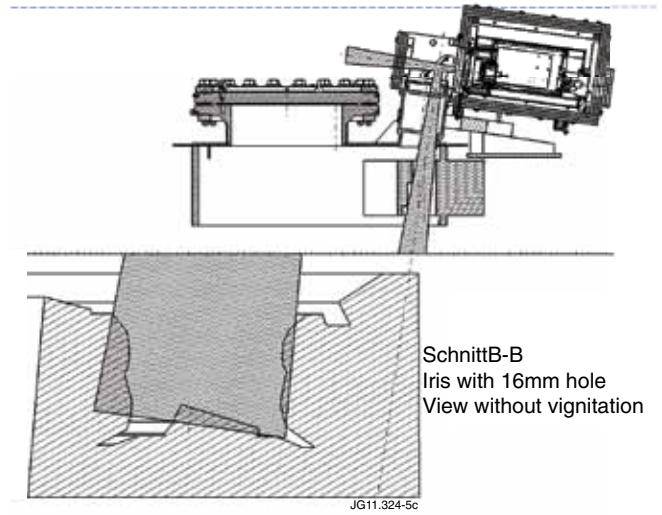
Figure 5: the IR camera located on top of JET and its field of view.
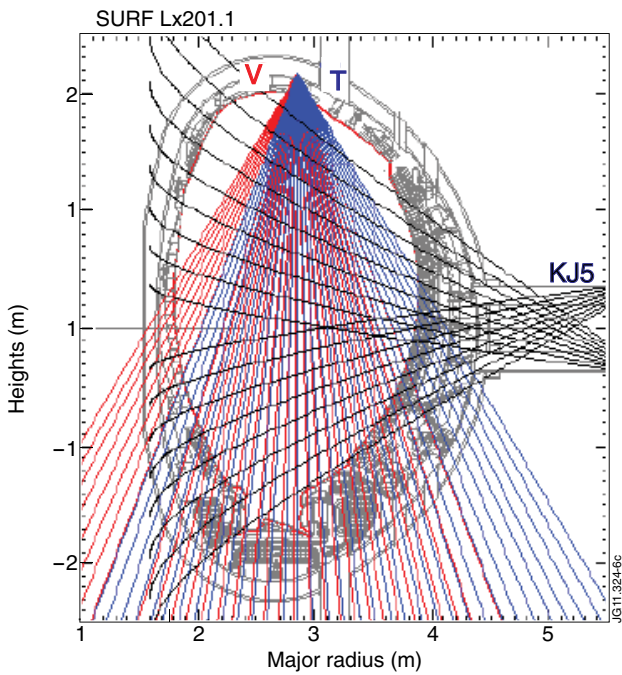
Figure 6: Lines of sight of the Si diodes in JET three main cameras.
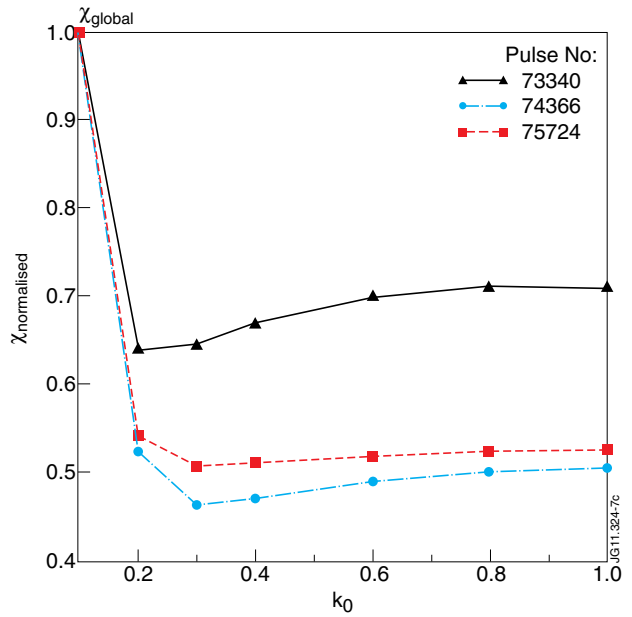
Figure 7: Behaviour of the normalized χ for the Pulse No's: 73340; 74366; 75724

16
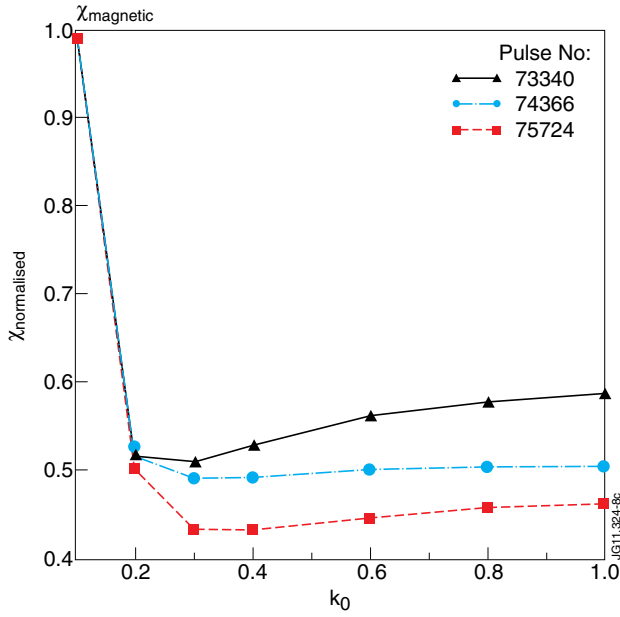
Figure 8: Normalized $\chi_{magnetic}$ computed using the magnetic measurements: pick-up coils, saddle coils and poloidal fluxes.
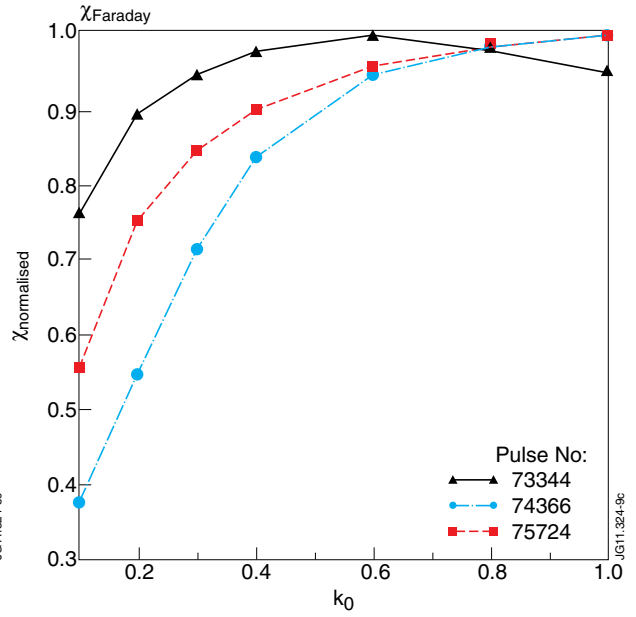
Figure 9: Normalized $\chi_{Faraday}$ computed using the Faraday measurements.
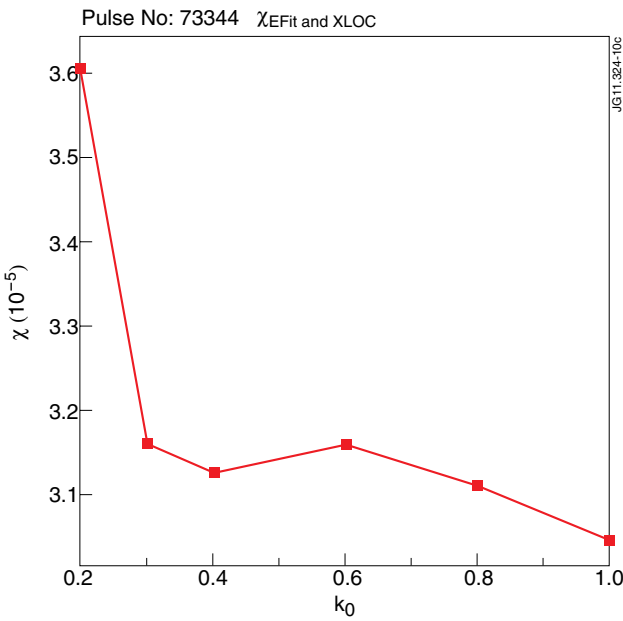
Figure 10: χ computed using the reconstruction of the EDGE done by EFIT and XLOC.
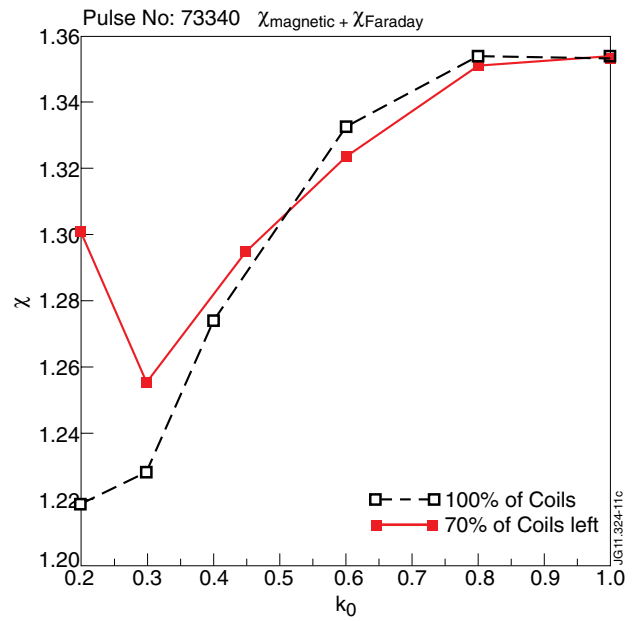
Figure 11: Pulse No: 73340. Eliminating 30% of the magnetic probes, the best parameter to be used become $K_0 = 0.3$ instead of 0.2.

17
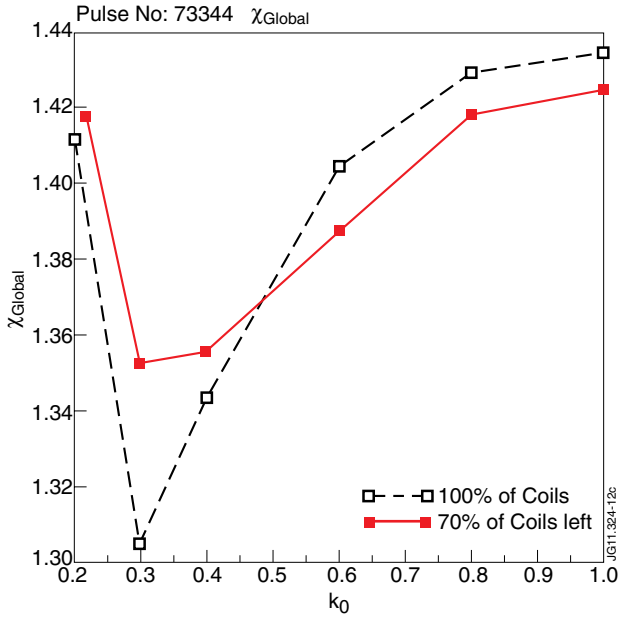
Figure 12: Pulse No: 73344. Eliminating 30% of the magnetic probes, χ has a minimum for both $K_0 = 0.3$ and $K_0 = 0.4$ instead of a clear minimum at $K_0 = 0.3$.
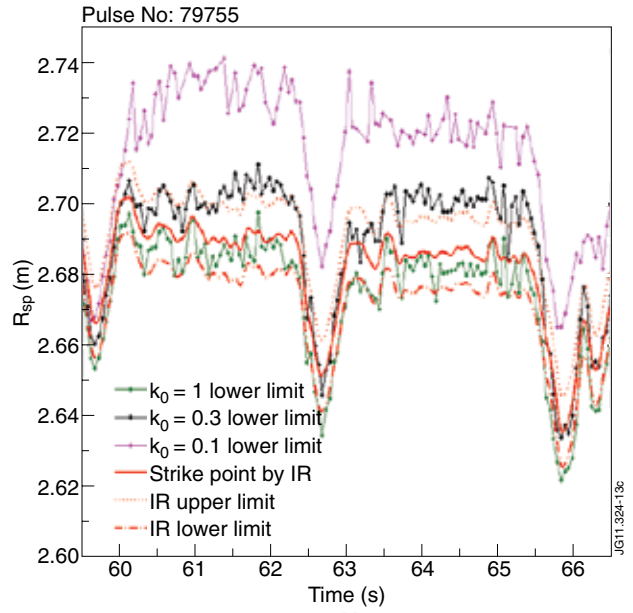
Figure 13: Pulse No: 79755. Position of the outer strike point identified by the IR camera. Both the upper and lower limits are shown. The lower limits of the strike point position indicated by EFIT for K_0 = {0.1, 0.3, 1} are also plotted.
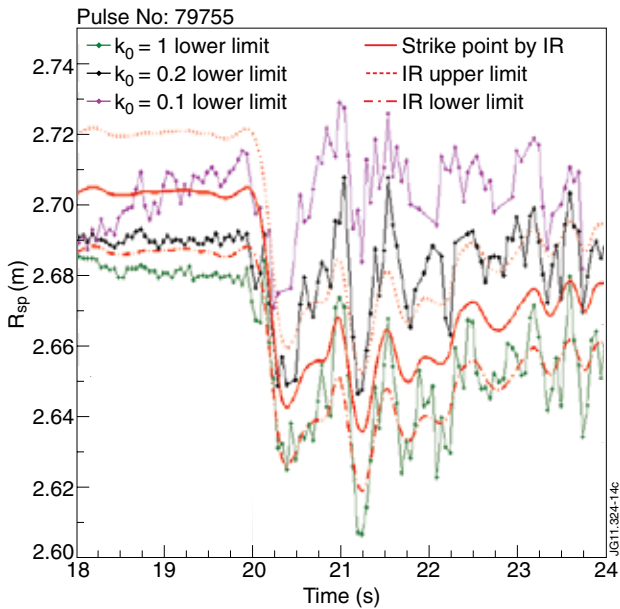
Figure 14: Pulse No: 79756. Position of the outer strike point identified by the IR camera. Both the upper and lower limits are shown. The lower limits of the strike point position indicated by EFIT for K_0 = {0.1, 0.2, 1} are also plotted.
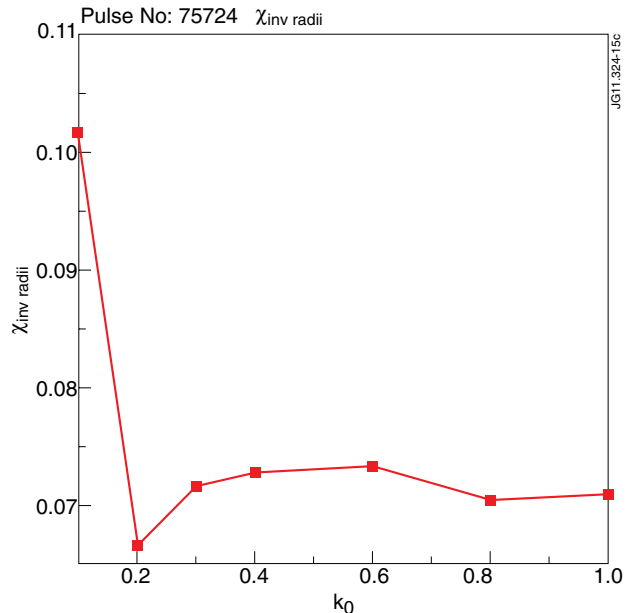
Figure 15: χ computed as the difference between the radial position of the rational surface using the EFIT profile and the SXR emission.

18